

Article

Research into Carbon Dioxide Curing's Effects on the Properties of Reactive Powder Concrete with Assembly Unit of Sulphoaluminate Cement and Ordinary Portland Cement

Hongfei Cao ^{1,2}, Zhao Liang ^{1,3}, Xi Peng ^{2,4}, Xin Cai ^{1,3}, Kewei Wang ^{1,3}, Hui Wang ^{1,3,*} and Zhongda Lyu ^{2,4,*}

¹ Faculty of Mechanical Engineering and Mechanics, Ningbo University, Ningbo 315211, China; caohongfei92@163.com (H.C.); liangzhao@aliyun.com (Z.L.); caixin@aliyun.com (X.C.); wangkewei@aliyun.com (K.W.)

² School of Civil and Transportation Engineering, Ningbo University of Technology, Ningbo, 315211, China; s7ilent@sina.com

³ School of Civil and Environmental Engineering, Ningbo University, Ningbo 315211, China

⁴ Engineering Research Center of Industrial Construction in Civil Engineering of Zhejiang, Ningbo University of Technology, Ningbo 315211, China

* Correspondence: huiwang123@aliyun.com (H.W.); lzd01@189.cn (Z.L.)

Abstract: Excessive emissions of carbon dioxide can lead to greenhouse effect thus destroying the ecological balance. Therefore, effective measures need to be taken to reduce the emission of carbon dioxide. In this study, the influence of carbon dioxide curing on the mechanical strength and NaCl freeze-thaw deterioration of reactive powder concrete (RPC) with the assembly unit of sulphoaluminate cement and ordinary Portland cement was investigated. The ratio of sulphoaluminate cement ranged from 0% to 100% by the total mass of cement with the curing age ranging from 1 d to 28 d. The mechanical strength of RPC with 50% ordinary Portland cement and 50% sulphoaluminate cement containing the polypropylene fibers ranging from 1% to 4% by volume of RPC were investigated. Moreover, the following mass and mechanical strength loss rates, the carbonation depth, the chloride ion migration coefficient and the relative dynamic elastic modulus (RDEM) during NaCl freeze-thaw cycles were determined. Finally, the scanning electron microscope (SEM) and X-ray diffraction were applied in investigating the carbonation process of RPC. Results showed that the addition of sulphoaluminate cement could improve the mechanical strength of RPC at low curing age (lower than 7 d). However, when the curing age reached 7 d, the sulphoaluminate cement demonstrated negative effect on the mechanical strength. Moreover, the carbon dioxide curing led to increases in the mechanical strength and when ordinary Portland cement was added the enhancing effect was more obvious. Furthermore, the carbon dioxide curing could effectively improve the resistance of NaCl freeze-thaw cycles and increase the carbonation depth. Finally, the increasing dosages of polypropylene fibers were advantageous to the mechanical strength and the resistance of NaCl freeze-thaw cycles. From the researching results of the microscopic performance, the carbon dioxide curing could improve the compactness of hydration products and reduce the content of calcium hydroxide especially at the curing age of 3 days.

Keywords: carbon dioxide curing; mechanical strength; NaCl freeze-thaw deterioration; mass loss; carbonation depth; the relative dynamic elastic modulus

Citation: Cao, H.; Liang, Z.; Peng, X.; Cai, X.; Wang, K.; Wang, H.; Lyu, Z. Research of Carbon Dioxide Curing on the Properties of Reactive Powder Concrete with Assembly Unit of Sulphoaluminate Cement and Ordinary Portland Cement. *Coatings* **2022**, *12*, 209. <https://doi.org/10.3390/coatings12020209>

Academic Editor: Paolo Castaldo

Received: 19 January 2022

Accepted: 3 February 2022

Published: 5 February 2022

Publisher's Note: MDPI stays neutral with regard to jurisdictional claims in published maps and institutional affiliations.



Copyright: © 2022 by the authors. Licensee MDPI, Basel, Switzerland. This article is an open access article distributed under the terms and conditions of the Creative Commons Attribution (CC BY) license (<http://creativecommons.org/licenses/by/4.0/>).

1. Introduction

Excessive emissions of carbon dioxide will destroy the atmospheric ozone layer and cause the greenhouse effect thus leading to increases in the temperature and affecting the living environment of human beings. It is necessary to draw down surplus carbon dioxide in time [1,2].

Cement concrete is a major construction material, which has been applied in the civil engineering field for many years [3,4]. Diversification of cement concrete materials has provided an innovative idea for the reasonable disposal of carbon dioxide [5,6]. The research of application of carbon dioxide in cement concrete buildings has been reported for several years [7,8]. This viewpoint was firstly put forward in 1970s and has become a research hotspot recently. As reported in some research, the CO₂ can be used for preparing lower carbon concrete and cement products [9,10]. Some journals pointed out that carbon dioxide curing could improve the mechanical properties and durability of cement concrete [11,12]. Ahmad found that the compressive strength of cement concrete cured in carbon dioxide for 1 day was 35–40% higher than that of cured in the standard curing environment [13,14]. Rostami [15] found that the compressive strength of cement paste cured in 8% carbon dioxide for 20 h was 40% higher than that obtained by normal hydration. Qin et al. [16] pointed out that the carbon dioxide curing can effectively improve the compressive strength and chloride ion permeability of cement paste with limestone powder, fly ash and ground granulated blast-furnace slag.

Although, several studies on carbon dioxide curing cement-based materials have been reported, little attention has been paid to the carbon dioxide curing methods on the high performance or ultra-high-performance concrete [17–19].

Reactive powder concrete (RPC) is a kind of high-performance concrete, which is produced based on the maximum density theory [20]. This type of cement concrete shows excellent mechanical strength and durability and has been applied in special engineering structures such as marine structures and precast pile foundation [21,22]. Bridges belong to the hub of transportation. Nowadays, sea-crossing bridges in coastal cities are frequently built, which are the hubs of transportation. The sea crossing bridge deck encounters complex environments and serious damage often occurs. Concrete is still the main material used in bridge construction. The cement concrete in sea-crossing bridges deteriorates frequently. In order not to delay the operation of bridges, the damaged part should be repaired rapidly [23]. Cai et al. [24] reported that the sulphoaluminate cement-based reactive powder concrete possessed mechanical strength after short term curing. Moreover, research has confirmed that the sulphoaluminate cement-based reactive powder concrete exhibited good resistance to chloride freeze-thaw cycles. Sulphoaluminate cement-based reactive powder concrete behaved good performance at earlier curing age (lower than 1 day). However, the latter's strength (strength curing for more than 28 days) is not ideal. Herein above statement, accelerating the strength growth of cement-based reactive powder concrete with carbon dioxide curing is very important. The Ordinary portland cement shows good later mechanical properties and durability, nevertheless, the early strength is low and is difficult for rapid repairing. Therefore, research of the carbon dioxide curing on resistance of reactive powder concrete with assembly unit of sulphoaluminate cement and ordinary Portland cement is necessary.

This paper aims to study the influence of carbon dioxide curing on the mechanical strength (flexural and compressive strength) and resistances of NaCl freeze-thaw cycles. The concentration of sodium chloride for the freeze-thaw cycles was 3%. The mass and mechanical strength loss rates and the relative dynamic elastic modulus and carbonation depth were determined to reflect the NaCl freeze-thaw damage. This research will provide an excellent method to deal with carbon dioxide in the future.

2. Experimental Section

2.1. Raw Materials

Polypropylene fibers supplied by Shanghai yiou Engineering Materials Co., Ltd., Shanghai, China, were selected for this study. The density, length and diameter of polypropylene fibers were 0.91 g/cm³, 10–13 mm, and 18–48 μm respectively. The corresponding aspect ratios, tensile strength and average elastic modulus of polypropylene fibers were 208–722, 710 and 3850 MPa. Polypropylene fibers used in this study possess

excellent acid and alkali resistance. The tabular form and the photos of the polypropylene fibers are shown in Table 1 and Figure 1 respectively.

Table 1. The basic performance indexes of polypropylene fibers.

| Density(g/cm ³) | Length (mm) | Diameter (μm) | Tensile Strength(MPa) | Modulus of Elasticity(GPa) |
|-----------------------------|-------------|---------------|-----------------------|----------------------------|
| 0.91 | 10–13 | 18–48 | 710 | 3.85 |



Figure 1. The polypropylene fibers.

RC.SAC fast hard sulphoaluminate cement (SAC), Ordinary Portland cement (OPC), and silica fume (SF) with the specific surface area of 15 m²/g, density of 2.2 g/cm³, specific surface area of 436 m²/g and the SiO₂ content exceeding 98% were used as one kind of mineral admixture. Additionally, granulated blast furnace slag powder (GGBS) with the density of 2.9 g/cm³ and the corresponding loss on ignition of 2.3% was applied as another mineral admixture. The manufacturers of fast hard sulphoaluminate cement and Ordinary Portland cement with the strength grade of 42.5 MPa were Tangshan Polar Bear Building Materials Co., Ltd., Tangshan, China and Harbin Qiangshi Concrete Technology Development Co., Ltd., Harbin, China, respectively. Quartz sand with 99.6% SiO₂, 0.02% Fe₂O₃ and other ingredients were used as the unique aggregate in this study. The sieving sizes of quartz sand were 1–0.71 mm, 0.59–0.35 mm and 0.15–0.297 mm and the corresponding mass ratios were 1:1.5:0.8. The mineral admixtures and quartz sand were manufactured by Lingshou Aihong mineral products Co., Ltd., Lingshou, China. Lithium sulfate and calcium formate with purities of 99.93% and 99.95% were used as early strength agents for SAC and OPC respectively. Tartaric acid with 99.9% purity was used for retarding of cement. All cement early strength agents and retarder agent were produced by Yingshan New Material Technology Co., Ltd., Shanghai China. Polycarboxylate superplasticizer with 40% water reduction rater provided by Henan Lichuang lier Technology Co., Ltd., Pingdingshan, China, was used to obtain fresh RPC with large fluidity. Tables 2 and 3 show the particle size distribution and chemical composition of cementitious materials respectively. The mixing proportion of RPC is shown in Table 3.

Table 2. Particle passing percentage of the cementitious materials (%).

| Types | Particle Size(μm) | | | | | | |
|-------------|-------------------|------|------|-------|-------|-------|-----|
| | 0.3 | 0.6 | 1 | 4 | 8 | 64 | 360 |
| SAC | 0 | 0.35 | 1.92 | 16.35 | 30.12 | 95.15 | 100 |
| P-O Cement | 0 | 0.33 | 2.66 | 15.01 | 28.77 | 93.59 | 100 |
| Slag power | 0.025 | 0.1 | 3.51 | 19.63 | 35.01 | 97.9 | 100 |
| Silica fume | 31.2 | 58.3 | 82.3 | 100 | 100 | 100 | 100 |

Table 3. Chemical composition of the cementitious materials (%).

| Types | SiO ₂ | Al ₂ O ₃ | Fe ₂ O ₃ | MgO | CaO | SO ₃ | Ti ₂ O |
|-------------|------------------|--------------------------------|--------------------------------|------|-------|-----------------|-------------------|
| SAC | 4.55 | 50.23 | 33.22 | 5.95 | 0.79 | 0.91 | 1.48 |
| OPC | 4.55 | 50.23 | 33.22 | 5.95 | 0.79 | 0.91 | 1.48 |
| Slag power | 42.19 | 27.56 | 15.80 | 0.31 | 7.52 | 2.89 | 0.45 |
| Silica fume | 48.62 | 29.67 | 0.72 | 0.47 | 20.17 | 0.05 | 0.18 |

2.2. Specimens Preparation

The manufacturing process of RPC specimens were carried out following these steps.

The SAC, OPC, SF, GGBS, quartz sand, polypropylene fibers, lithium sulfate and calcium formate were added in the UJZ-15 mortar mixer and mixed for 1 min. Then, the water-reducing agent is mixed with water, then the mixed solution was added in the mixture and stirred for the last 5 min. The slump flow of fresh RPC was 210–230 mm. The mix proportion of RPC is shown in Table 4.

Table 4. Mix proportions of RPC per one cubic meter (kg).

| Specimens | Water | OPC | SAC | SF | GGBS | Quartz Sand | Water-Reducer | PPFs | Li ₂ SO ₄ | Tartaric Acid | Calcium Formate |
|-----------|-------|-------|-------|-------|-------|-------------|---------------|------|---------------------------------|---------------|-----------------|
| RPC-1 | 244.4 | 740.7 | 0 | 370.3 | 111.1 | 977.9 | 16.3 | 0 | 0 | 0 | 5.2 |
| RPC-2 | 244.4 | 555.5 | 185.2 | 370.3 | 111.1 | 977.9 | 16.3 | 0 | 1.3 | 0.3 | 3.9 |
| RPC-3 | 244.4 | 370.4 | 370.4 | 370.3 | 111.1 | 977.9 | 16.3 | 0 | 2.6 | 0.6 | 2.6 |
| RPC-4 | 244.4 | 185.2 | 555.5 | 370.3 | 111.1 | 977.9 | 16.3 | 0 | 3.9 | 0.8 | 1.3 |
| RPC-5 | 244.4 | 0 | 740.7 | 370.3 | 111.1 | 977.9 | 16.3 | 0 | 5.2 | 1.1 | 0 |
| RPC-6 | 244.4 | 370.4 | 370.4 | 370.3 | 111.1 | 977.9 | 16.3 | 0.91 | 2.6 | 0.6 | 2.6 |
| RPC-7 | 244.4 | 370.4 | 370.4 | 370.3 | 111.1 | 977.9 | 16.3 | 1.82 | 2.6 | 0.6 | 2.6 |
| RPC-8 | 244.4 | 370.4 | 370.4 | 370.3 | 111.1 | 977.9 | 16.3 | 2.73 | 2.6 | 0.6 | 2.6 |
| RPC-9 | 244.4 | 370.4 | 370.4 | 370.3 | 111.1 | 977.9 | 16.3 | 3.64 | 2.6 | 0.6 | 2.6 |

2.3. Measurement Methods

Specimens with a size of 40 mm × 40 mm × 160 mm were selected for the measurement of mechanical strength. Meanwhile, the specimens with size of 100 mm × 100 mm × 400 mm and 100 mm × 100 mm × 100 mm were applied for the determination of relative dynamic modulus of elasticity (RDME) of NaCl freeze-thaw cycles and the carbonation depth respectively. Two different curing methods (one curing method was temperature of 20 ± 2 °C and relative humidity of above 95%, and the other curing method was 10% CO₂ and 90% air) were used for curing the specimens. All specimens were cured in the curing environment for 1 day before demolding. After demolding, the specimens were cured for the corresponding curing age. The NaCl freeze-thaw cycles were implemented following these steps.

The specimens were immersed in the sodium chloride solution for 4 days after curing in standard curing environment or CO₂ environment for 24 days. After this step, the specimens were moved to a stainless steel sealed casing filled with 3% NaCl solution for rapid freeze-thaw experiments. The temperature for rapid freeze-thaw cycles of RPC ranged from −15 °C to 8 °C. The NaCl solution on the surface of specimens was wiped off by a twisted rag per 50 NaCl freeze-thaw cycles. After this step, the mass of all specimens were tested and the mass loss rate was calculated. The RDME was tested by the DT-20 dynamic elastic modulus tester produced by Cangzhou Huaheng Test Instrument Co., Ltd., Cangzhou, China. For measuring the RDME, a detector was stick to the center of the specimen by vaseline, another detector was attached to the axis 5 mm away from the end of the specimen. The positions of the detectors during the measuring of RDME are shown in Figure 2. The testing process of the RDME is shown in Figure 1. Specimens with size of

Φ 100 mm \times 100 mm were used for the measurement of chloride ion migration coefficient (CMC) of RPC. Durable Albert electromigration concrete chloride ion diffusion coefficient tester manufactured by Cangzhou Yixuan Test Instrument Co., Ltd., Cangzhou, China was applied in testing CMC. All experiments were carried out refer to the Chinese Standard GB/T 50082-2009 [25].

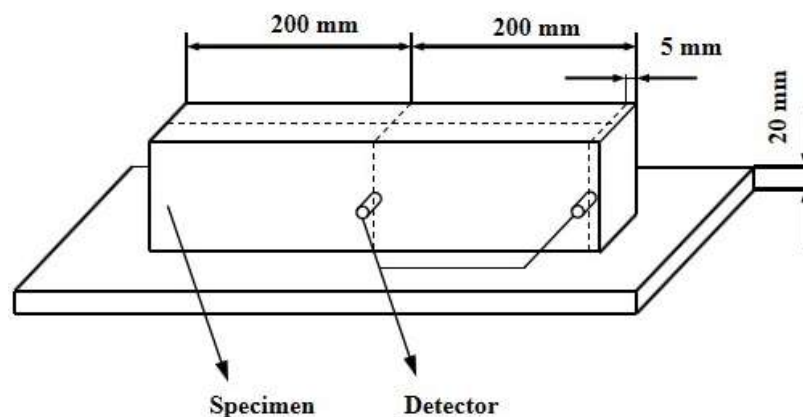


Figure 2. The positions of the detectors during the measuring of RDME.

The mechanical strength of the RPC were performed by using the YAW-300 micro-computer full-automatic universal tester with the maximum testing force of 300 kN manufactured by Henruijin Co., Ltd., Jinan, China. This experiment was conducted according to GB/T 17671-1999 Chinese standard [26]. Three specimens were prepared for each experiment.

3. Results and Discussion

3.1. Mechanical Strength

The mechanical strength (the flexural and compressive strength) of RPC are illustrated in Figure 3. The cement applied in manufacturing RPC was composed of OPC and SAC. The samples were cured in standard curing environment. It can be obtained from Figure 3, the mechanical strength increased obviously with the increasing curing age, due to the improvement of cement hydration degree [27]. The increasing dosage of SAC led to increasing the mechanical strength at low curing age (lower than 7 days). However, the mechanical strength decreased with the increasing content of SAC when the curing age was higher than or equal to 7 days. This was attributed to the fact that the SAC could effectively accelerate the cement hydration speed and improve the mechanical strength. However, when the curing age was higher than or equal to 7 days, the addition of SAC demonstrated negative effect on the mechanical strength of RPC. As reported in other research [28], OPC with the curing age higher than 7 days showed better performance than SAC. Therefore, the mechanical strength of RPC with OPC at these curing times were better. Comparing the research findings with previous studies, the mechanical strength of RPC with blended cement (OPC and SAC) was lower than the RPC with SAC when the curing age was lower than 3 days. However, when the curing age exceeded 3 days, RPC with blended cement showed better mechanical properties [21].

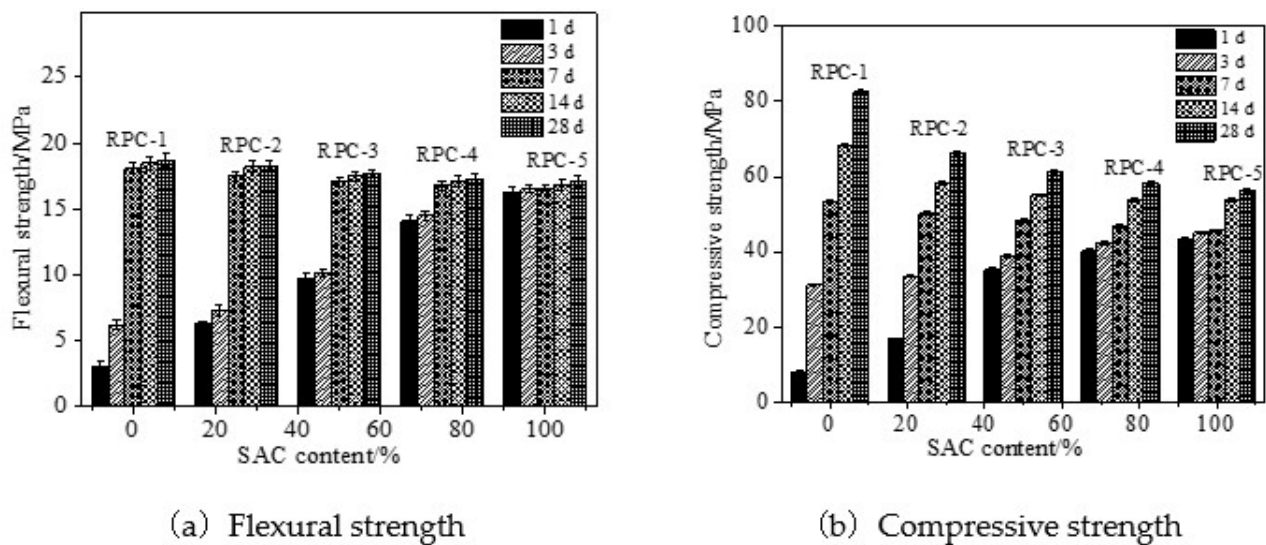


Figure 3. Mechanical strength of RPC cured in standard curing environment.

Figure 4 shows the mechanical strength of RPC cured in the carbon dioxide. It can be seen in Figure 4 that the mechanical strength of RPC increased with the increasing curing time by carbon dioxide. With the same increasing curing time, the mechanical strength of RPC demonstrated the similar law with that of RPC cured in standard curing environment. It can be obtained by comparing Figures 3 and 4, the mechanical strength of RPC cured in carbon dioxide was higher than that cured in standard curing environment. This was attributed to the fact that the carbon dioxide reacted with alkaline substances and formed carbonate thus increasing the compactness and reducing the porosity of RPC leading eventually to improving the mechanical strength [29].

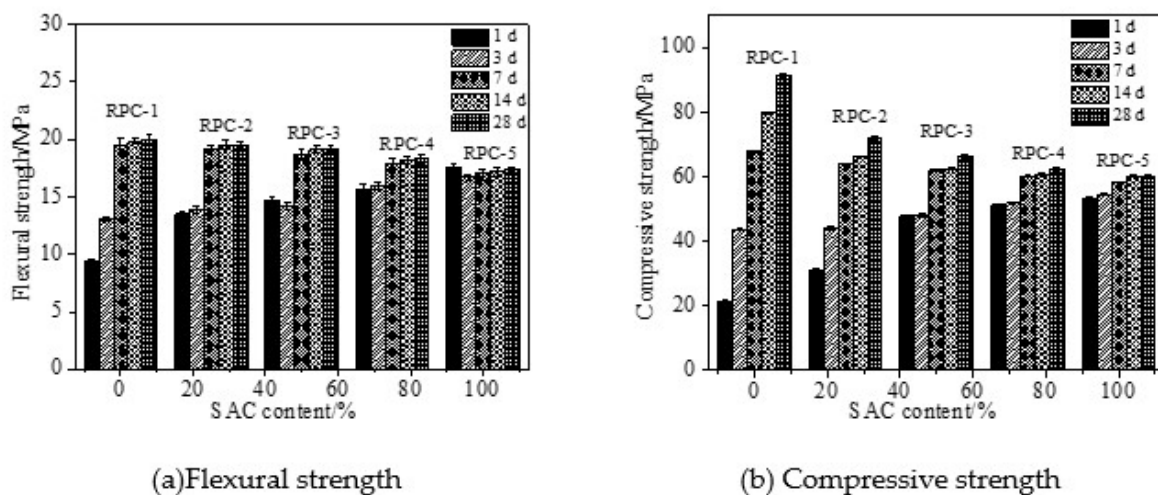


Figure 4. Mechanical strength of RPC cured in carbon dioxide curing environment.

Figure 5 shows the increasing rate of mechanical strength of RPC cured in carbon dioxide compared with the specimens cured in standard curing environment. As obtained from Figure 5, the increasing rate of mechanical strength of RPC decreased with the curing age and the increasing dosages of SAC. Due to the fact that the alkaline substance of SAC was lower than that of OPC, therefore, the reaction degree of carbon dioxide of RPC with higher dosage of SAC decreased, hence the following mechanical strength was lower. Finally, it can be observed in Figure 5, that the increasing rate of flexural strength was higher than that of compressive strength. Compared with the

standard curing, the carbon dioxide curing could increase the mechanical strength of RPC by 25–213% when the curing age was 1 day. However, when the curing age was equal to or higher than 3 day, the increasing rates were 8.6–112.1%.

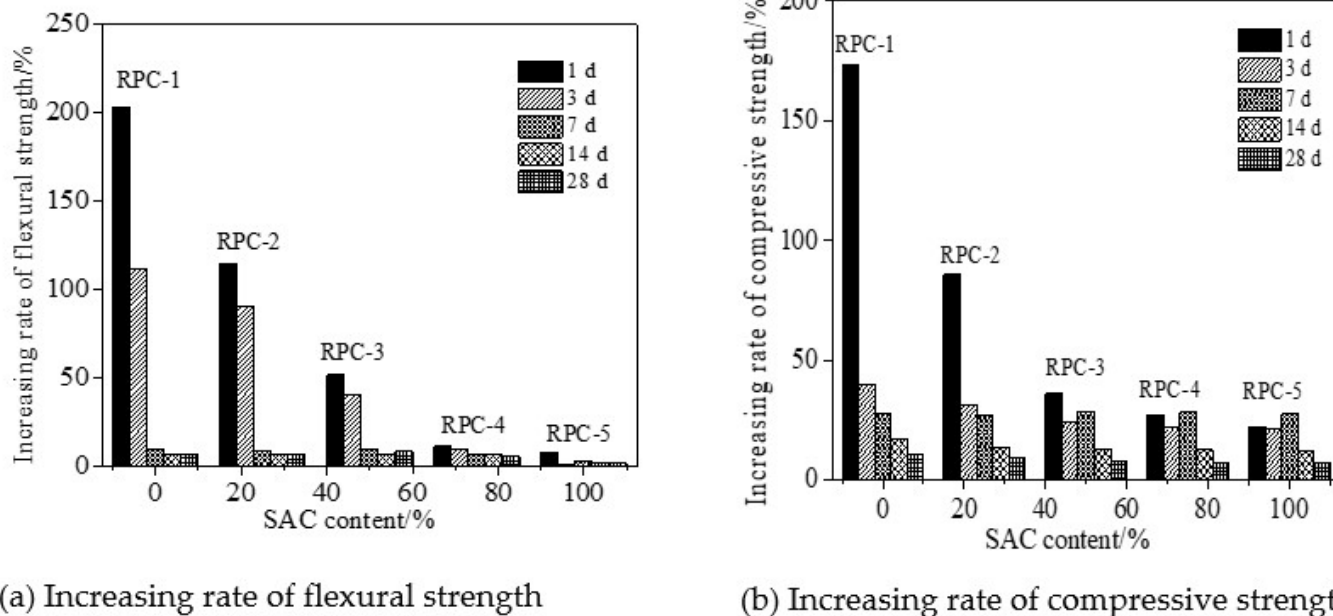


Figure 5. Increasing rates of mechanical strength of RPC by carbon dioxide curing environment.

3.2. Mechanical Properties of RPC during NaCl Freeze-Thaw Cycles

In this part, the RPC contained 50% SAC and 50% OPC by the mass ratio of the total cement. Figure 6 shows the mass loss rate of RPC during NaCl freeze-thaw cycles. As depicted in Figure 6, the mass loss rate increased with the increasing number of NaCl freeze-thaw cycles due to the fact that the frost heaving stress could induce the inner cracks of RPC resulting in increasing the spalling on the surface of RPC and decreasing the following mass. As observed from Figure 6, the mass loss rate decreased by the increasing dosage of polypropylene fibers due to the limited cracks propagation of RPC, thus decreasing the mass loss of RPC. Moreover, the carbon dioxide curing could reduce the mass loss due to the fact that the carbon dioxide curing could improve the porosity of RPC thus limiting the expansion of inner cracks during NaCl freeze-thaw cycles [30].

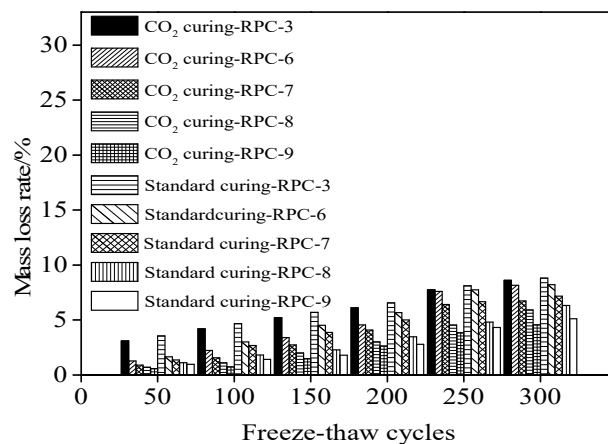


Figure 6. The mass loss rate of RPC during NaCl freeze-thaw cycles.

The relative dynamic modulus of elasticity of RPC during NaCl freeze-thaw cycles is shown in Figure. As illustrated in Figure 7, the relative dynamic modulus of elasticity decreased in the form of quadratic function with the increasing number of NaCl freeze-thaw cycles. This was attributed to the fact that the NaCl freeze-thaw cycles could accelerate the crack propagation of RPC, thus hindering the transmission of sound and decreasing the relative dynamic modulus of elasticity [31,32]. As shown in Figure 7, the increasing dosages of polypropylene fibers demonstrated a positive effect on the relative dynamic modulus of elasticity due to the limiting effect of polypropylene fibers on crack propagation. Therefore, the relative dynamic modulus of elasticity increased with the increasing content of polypropylene fibers. Furthermore, the carbon dioxide curing could increase the relative dynamic modulus of elasticity during NaCl freeze-thaw cycles [33]. Table 5 shows the fitting results of the RDEM and the number of freeze-thaw cycles (N). It can be deduced from Table 5 that the fitting degree of the fitting equations was higher than 0.92 indicating the accuracy of fitting equation.

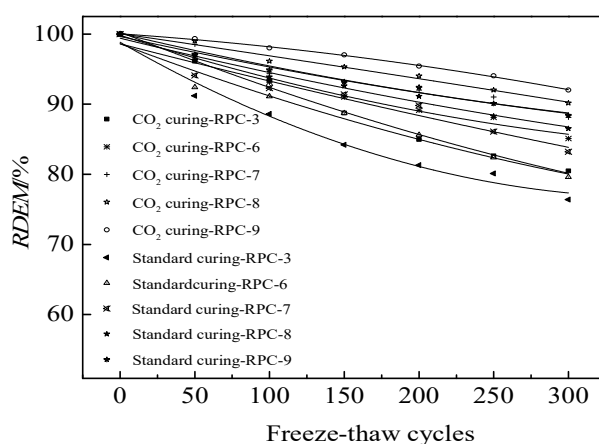


Figure 7. The RDEM during NaCl freeze-thaw cycles.

Table 5. The fitting results of the RDEM and the number of freeze-thaw cycles (N).

| Equation | Curing Type | Fiber Content/% | a | b | c | R ² |
|------------------------|------------------------|-----------------|------------------------|--------|--------|----------------|
| $RDEM = aN^2 + bN + c$ | Standard curing | 0 | 5.90×10^{-5} | -0.085 | 100.29 | 0.99 |
| | | 1 | 6.98×10^{-5} | -0.068 | 99.82 | 0.98 |
| | | 2 | 4.30×10^{-5} | -0.051 | 100.09 | 0.95 |
| | | 3 | -4.33×10^{-6} | -0.031 | 100.07 | 0.98 |
| | | 4 | -3.97×10^{-5} | -0.015 | 100.04 | 0.99 |
| | | 0 | 1.69×10^{-4} | -0.122 | 98.83 | 0.97 |
| | CO ₂ curing | 1 | 6.24×10^{-5} | -0.081 | 98.61 | 0.95 |
| | | 2 | 1.95×10^{-5} | -0.055 | 98.61 | 0.92 |
| | | 3 | 3.41×10^{-5} | -0.052 | 99.41 | 0.98 |
| | | 4 | 3.48×10^{-5} | -0.047 | 99.66 | 0.98 |

Figure 8 shows the flexural and compressive strength loss rate of RPC. As depicted from Figure 8, the mechanical strength loss rate decreased with the increasing number of NaCl freeze-thaw cycles and carbon dioxide curing. Moreover, the carbon dioxide curing on RPC led to decreasing the mechanical strength loss rate of RPC, due to the fact that the internal pores of RPC were filled by the carbonation products leading to improvement of the following mechanical performances [34]. Moreover, the flexural strength loss rate was higher than that of the compressive strength loss rate.

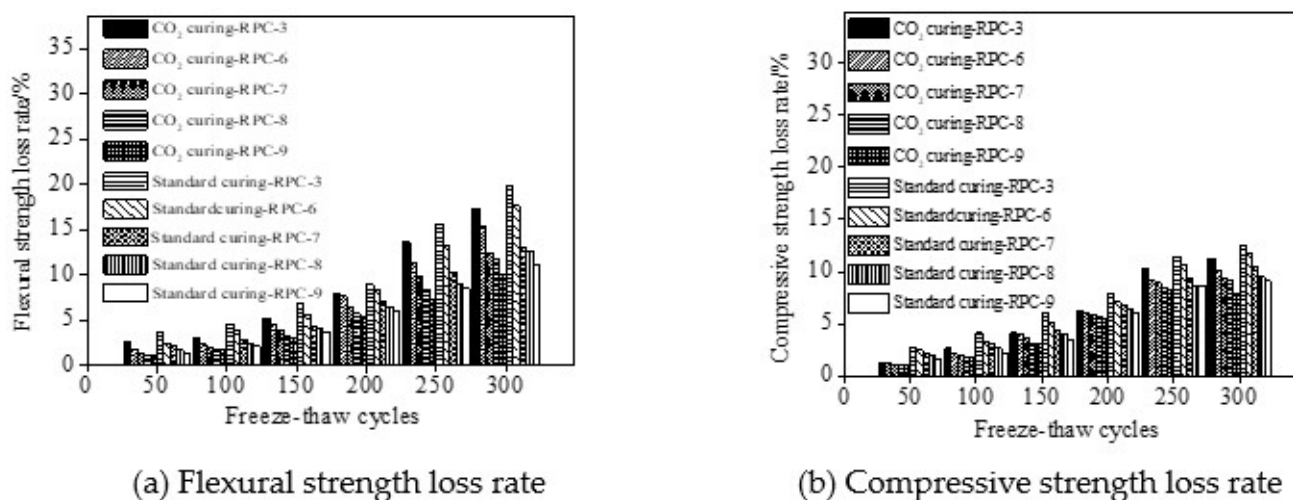


Figure 8. Mechanical strength loss rates of RPC during NaCl freeze-thaw cycles.

Figure 9 shows the carbonation depth of RPC during NaCl freeze-thaw cycles. RPC-3, RPC-6, RPC-7, RPC-8 and RPC-9 corresponding to polypropylene fibers of 1%, 2%, 3% and 4% by the volume of RPC were selected. It can be observed from Figure 9, the carbonation depth of RPC increased with the increasing number of NaCl freeze-thaw cycles and carbon dioxide curing. This was attributed to the fact that the NaCl freeze-thaw cycles could lead to accelerated propagation of internal cracks. Therefore, more internal alkaline substances reacted with carbon dioxide leading to increase in the carbonation depth [35]. Moreover, the carbon dioxide reacted with alkaline substances thus resulting in the carbonation degree and increasing the carbonation depth [36]. Additionally, the increasing dosages of polypropylene fiber could limit internal crack extension and propagation, thus decreasing the carbonation depth of RPC [24].

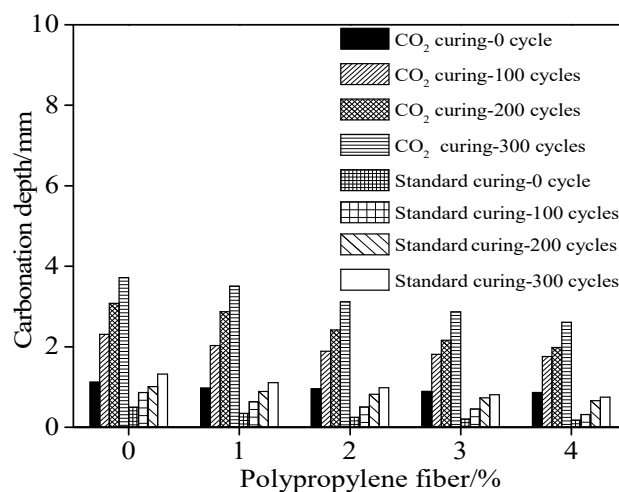


Figure 9. Carbonation depth of RPC during different NaCl freeze-thaw cycles.

Figure 10 shows the chloride migration coefficient (CMC) of RPC cured in the standard curing environment and carbon dioxide curing environment respectively. The CMC was determined per 50 NaCl freeze-thaw cycles. As illustrated in Figure 10, the CMC increased in the form of quadratic function with the number of NaCl freeze-thaw cycles. This was attributed to the fact that the NaCl freeze-thaw cycles could accelerate crack propagation of inner RPC, thus speeding up the migration of chloride ions, leading eventually to increase in the CMC of RPC [37]. As depicted in Figure 10, the CMC

was decreased by the increasing dosages of polypropylene fibers due to the fact that the cracks propagation is restricted by polypropylene fibers thus preventing the migration of chloride ions and decreasing the CMC [24]. Furthermore, the CMC was reduced by carbon dioxide curing due to the reduced pore volume and pore size [38]. Table 6 shows the fitting results of the CMC and the number of freeze-thaw cycles (N). As Table 6 shows, the fitting degrees of all curves were 0.99, confirming the accuracy of the fitting functions. Comparing the researching results in this study and Ref [20], the NaCl freeze-thaw resistance of RPC with assembly unit of SAC and OPC was better than RPC with SAC. Moreover, RPC showed better NaCl freeze-thaw resistance when cured in the carbon dioxide than cured in standard curing environment.

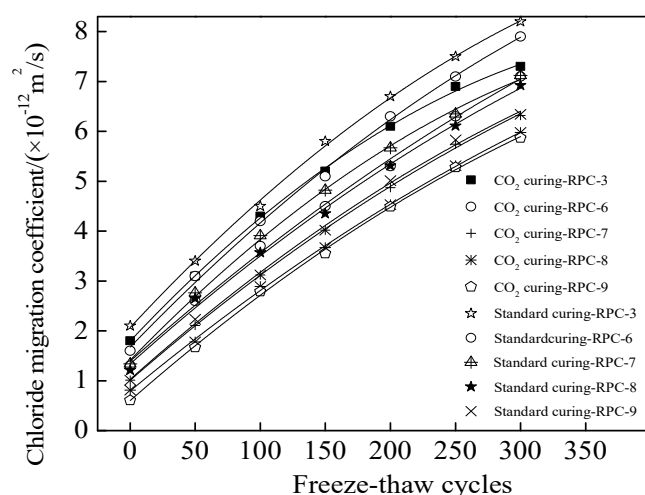


Figure 10. The chloride migration coefficient during NaCl freeze-thaw cycles.

Table 6. The fitting results of the CMC and the number of freeze-thaw cycles (N).

| Equation | Curing Type | Fiber content/% | a | b | c | R ² |
|-----------------------|------------------------|-----------------|------------------------|-------|------|----------------|
| $CMC = aN^2 + bN + c$ | Standard curing | 0 | -3.10×10^{-5} | 0.028 | 1.80 | 0.99 |
| | | 1 | -1.43×10^{-5} | 0.023 | 1.39 | 0.99 |
| | | 2 | -1.62×10^{-5} | 0.023 | 1.01 | 0.99 |
| | | 3 | -1.42×10^{-6} | 0.022 | 0.80 | 0.99 |
| | | 4 | -1.73×10^{-5} | 0.023 | 0.60 | 0.99 |
| | | 0 | -2.52×10^{-4} | 0.028 | 2.07 | 0.99 |
| | CO ₂ curing | 1 | -2.10×10^{-5} | 0.027 | 1.67 | 0.99 |
| | | 2 | -2.72×10^{-5} | 0.027 | 1.41 | 0.99 |
| | | 3 | -1.61×10^{-5} | 0.023 | 1.34 | 0.99 |
| | | 4 | -1.77×10^{-5} | 0.023 | 1.03 | 0.99 |

3.3. Microscopic Analysis

The blank RPC with 50% SAC and 50% OPC by the mass ratio of the total cement were used for the determination of microcosmic performance experiments. The mixing proportions of the microscopic experiments correspond to RPC-3. As the major product of concrete after carbonation is the formation of calcium carbonate, scanning electron microscopy (SEM) was adopted to investigate the microstructure of RPC after carbonation. Figure 11 shows the SEM photos of blank RPC cured in standard curing environment and carbon dioxide curing environment for 28 days. As shown in Figure 11, the microstructure of blank RPC after standard curing mainly comprised of needlelike and flocculent hydration products. After carbonation curing, RPC exhibited remarkable differences in the microstructure. Specifically, the needlelike structures almost vanished, and the small particles deposited on the cement matrix were belonging to the formation

of calcium carbonate particles. Since the carbon dioxide reacts with calcium hydroxide in concrete to form calcium carbonate when the specimens were cured in carbon dioxide environment, the formation and growth of calcium carbonate will result in forming dense structures inside the concrete [1,2]. Therefore, the pore structure was modified after carbonation curing. This phenomenon reflects that the RPC cured in carbon dioxide will exhibit a more compact microstructure and higher mechanical strength.



(a) Standard curing



(b) Carbon dioxide curing

Figure 11. SEM microstructure photos of RPC.

The X-ray diffraction (XRD) pattern photos of blank RPC specimens cured in carbon dioxide for 1 day, 3 days and 28 days respectively were shown in Figure 12. As shown in Figure 12, the diffraction peaks of $3\text{CaO}\cdot\text{SiO}_2$ (C_3S), $2\text{CaO}\cdot\text{SiO}_2$ (C_2S), cristobalite (SiO_2), $\text{Ca}(\text{OH})_2$ (CH) and CaCO_3 can be found in the curves. When the carbon dioxide curing time increased from 1 day to 3 days, the diffraction peaks $\text{Ca}(\text{OH})_2$ decreased obviously due to the fact that the carbon dioxide reacted with the inner $\text{Ca}(\text{OH})_2$ of RPC and then CaCO_3 formed [11]. This confirmed the result that when the carbon dioxide curing time increased from 1 day to 3 days, the strength of RPC increased rapidly. However, when the carbon dioxide curing time increased from 3 days to 28 days, small decline occurred to the diffraction peaks height of $\text{Ca}(\text{OH})_2$ due to the fact that most carbonization of RPC accomplished within 3 days. Therefore, the mechanical strength of RPC increased slowly when the carbon dioxide curing time increased from 3 days to 28 days.

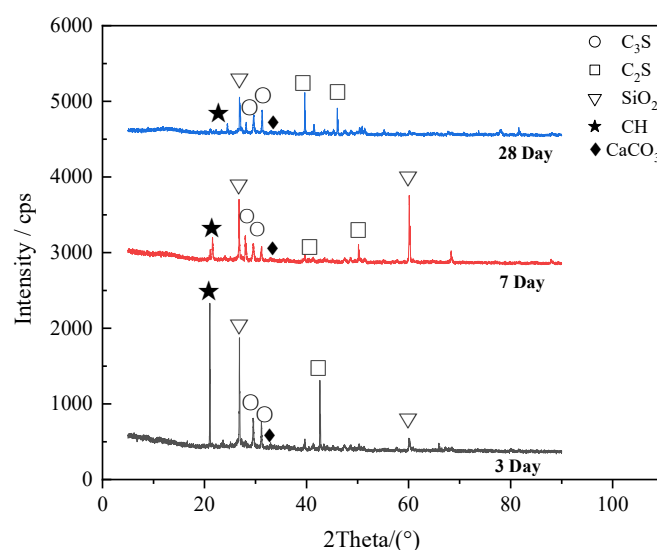


Figure 12. X-ray diffraction patterns of specimens.

4. Conclusions

In this study, the influence of carbon dioxide curing on the mechanical strength (flexural and compressive strength) and NaCl freeze-thaw resistance of reactive powder concrete (RPC) with assembly unit of sulphoaluminate cement and ordinary Portland cement were systematically investigated. Based on all experimental results, the conclusions can be summarized as follows:

The addition of sulphoaluminate cement could effectively improve the mechanical strength of RPC at early curing age (lower than 7 d) and demonstrated negative effect on the mechanical strength at later curing age (higher than or equal to 7 d).

Carbon dioxide curing and the increasing dosages of polypropylene fibers had a positive effect on the mechanical strength (flexural and compressive strength) and NaCl freeze-thaw resistance of RPC. When the content of ordinary Portland cement was higher, the enhancing effect was more obvious. However, the carbon dioxide curing led to increase in the carbonation depth of RPC. Carbon dioxide curing could increase the mechanical strength of RPC by 25~213% compared with that of standard curing when the curing age was 1 d. However, when the curing age was equal to or higher than 3 d, the increasing rates were 8.6~112.1%.

The relative dynamic modulus of elasticity and the chloride migration coefficient of RPC demonstrated a quadratic function relation with the increasing number of NaCl freeze-thaw cycles. In summary, carbon dioxide curing can effectively improve the mechanical properties and durability of RPC.

The experimental results of microscopic properties indicated that the carbon dioxide curing can improve the compactness of hydration products and reduce the content of calcium hydroxide especially at the curing age of 3 days.

Author Contributions: Conceptualization, H.C.; H.W. and Z.L.; methodology, X.C.; software, X.P.; validation, H.C. and Z.L.; formal analysis, H.W. and Z.L.; investigation, X.C.; resources, Y.L.; and H.W.; data curation, H.W. and H.C.; writing—original draft preparation, H.W.; Z.L.; H.C. and X.C.; writing—review and editing, H.W.; visualization, Z.L.; supervision, H.C.; K.W. and Y.L. project administration, Y.L.; and H.W.; funding acquisition, H.C.; X.C.; and K.W.; All authors have read and agreed to the published version of the manuscript.

Funding: This research was funded by the major special science and technology project of “Ningbo science and technology innovation 2025” [No. 2019B10076](Z.L.), the Zhejiang Provincial Natural Science Foundation [No. Y22E081344] and the National Natural Science Foundation of China [No. 51808300](H.W.).

Institutional Review Board Statement: Not applicable.

Informed Consent Statement: Not applicable.

Data Availability Statement: The data used to support the findings of this study are available from the corresponding author upon request.

Conflicts of Interest: The authors declare that there are no conflicts of interest regarding the publication of this paper.

References

1. Berger, R.; Young, J.; Leung, K. Acceleration of hydration of calcium silicates by carbon dioxide treatment. *Nature* **1972**, *240*, 16–18.
2. Goodbrake, C.; Young, J.; Berger, R. Reaction of hydraulic calcium silicates with carbon dioxide and water. *J. Am. Ceram. Soc.* **1979**, *62*, 488–491.
3. Shah, J. Laboratory characterization of controlled low-strength material and its application to construction of flexible pipe drainage system. *Health Manpow. Manag.* **2000**, *19*, 30–59.
4. Haselbach, L.; Valavala, S.; Montes, F. Permeability predictions for sand clogged Portland cement pervious concrete pavement systems. *J. Environ. Manag.* **2005**, *81*, 42–49.
5. Shtepenko, O.; Hills, C.; Brough, A.; Thomas, M. The effect of carbon dioxide on β -dicalcium silicate and Portland cement. *Chem. Eng. J.* **2006**, *118*, 107–118.
6. Grounds, T.; Midgley, H.; Novell, D. Carbonation of ettringite by atmospheric carbon dioxide. *Thermochim. Acta* **1988**, *135*, 347–352.
7. Mahoutian, M.; Ghouleh, Z.; Shao, Y. Carbon dioxide activated ladle slag binder *Constr. Build. Mater.* **2014**, *66*, 214–221.
8. Rendek, E.; Ducom, G.; Germain, P. Carbon dioxide sequestration in municipal solid waste incinerator (MSWI) bottom ash. *J. Hazard. Mater.* **2006**, *128*, 73–79.
9. Diener, S.; Andreas, L.; Herrmann, I.; Ecke, H.; Lagerkvist, A. Accelerated carbonation of steel slags in a landfill cover construction. *Waste. Manag.* **2010**, *30*, 132–139.
10. Gunning, P.; Hills, C.; Carey, P. Accelerated carbonation treatment of industrial wastes. *Waste. Manag.* **2010**, *30*, 1081–1090.
11. Monkman, S.M.; Macdonald, M. On carbon dioxide utilization as a means to improve the sustainability of ready-mixed concrete. *J. Clean. Prod.* **2017**, *167*, 365–375.
12. Smirnov, V.G.; Manakov, A.Y.; Dyrdin, V.V.; Ismagilov, Z.R.; Mikhailova, E.S.; Rodionova, T.V. The formation of carbon dioxide hydrate from water sorbed by coals. *Fuel* **2018**, *228*, 123–131.
13. Ahmad, S.; Assaggaf, R.; Maslehuddin, M.; Al-Amoudi, O.; Adekunle, S.; Ali, S.I. Effects of carbonation pressure and duration on strength evolution of concrete subjected to accelerated carbonation curing. *Constr. Build. Mater.* **2017**, *136*, 565–573.
14. Rostami, V.; Shao, Y.; Boyd, A.J. Carbonation curing versus steam curing for precast concrete production. *J. Mater. Civ. Eng.* **2011**, *24*, 1221–1229.
15. El-Hassan, H.; Shao, Y. Early carbonation curing of concrete masonry units with Portland limestone cement. *Cem. Concr. Compos.* **2015**, *62*, 168–177.
16. Qin, L.; Gao, X.; Chen, T. Influence of mineral admixtures on carbonation curing of cement paste. *Constr. Build. Mater.* **2019**, *212*, 653–662.
17. Ashraf, W. Carbonation of cement-based materials: Challenges and opportunities. *Constr. Build. Mater.* **2016**, *120*, 558–570.
18. Ashraf, W.; Olek, J. Carbonation behavior of hydraulic and non-hydraulic calcium silicates: Potential of utilizing low-lime calcium silicates in cement-based materials. *J. Mater. Sci.* **2016**, *51*, 6173–6191.
19. Morandea, A.E.; White, C.E. In situ X-ray pair distribution function analysis of accelerated carbonation of a synthetic calcium–silicate–hydrate gel. *J. Mater. Chem. A* **2015**, *3*, 8597–8605.
20. Mo, A.; El-Tawil, S.; Liu, Z.; Hansen, W. Effects of silica powder and cement type on durability of ultra-high performance concrete (UHPC). *Cem. Concr. Compos.* **2016**, *66*, 47–56.
21. Hong, H.; Wang, H.; Shi, F. Influence of NaCl Freeze Thaw Cycles and Cyclic Loading on the Mechanical Performance and Permeability of Sulphoaluminate Cement Reactive Powder Concrete. *Coatings* **2020**, *10*, 1227.

22. Mo, Z.; Gao, X.; Su, A. Mechanical performances and microstructures of metakaolin contained UHPC matrix under steam curing conditions. *Constr. Build. Mater.* **2021**, *268*, 121112.
23. Huang, G.; Wang, H.; Shi, F. Coupling Effect of Salt Freeze-thaw Cycles and Carbonation on the Mechanical Performance of Quick Hardening Sulphoaluminate Cement-based Reactive Powder Concrete with Basalt Fibers. *Coatings* **2021**, *11*, 1142.
24. Cai, Z.; Wang, H. Influence of NaCl Freeze-thaw Cycles on the Mechanical Strength of Reactive Powder Concrete with the Assembly Unit of Sulphoaluminate Cement and Ordinary Portland Cement. *Coatings* **2021**, *11*, 1238.
25. GB/T 50082-2009; Standard for Test Method of Long-Term Performance and Durability of Ordinary Concrete. Ministry of Housing and Urban Rural Development of the People's Republic of China: Beijing, China, 2009.
26. GB/T 17671-1999; Method of Testing Cements—Determination of Strength. The State Bureau of Quality and Technical Supervision: Beijing, China, 1999.
27. Velazco, G.; Almanza, J.M.; Cortés, D.A.; Escobedo, J.C.; Escalante-Garcia, J.I. Effect of citric acid and the hemihydrate amount on the properties of a calcium sulphoaluminate cement. *Mater. Constr.* **2014**, *64*, 1–8.
28. Liu, Y.; Tian, W.; Wang, M.; Qi, B.; Wang, W. Rapid strength formation of on-site carbon fiber reinforced high-performance concrete cured by ohmic heating. *Constr. Build. Mater.* **2020**, *244*, 118344.
29. Huijgen, W.J.; Witkamp, G.J.; Comans, R.N. Mechanisms of aqueous wollastonite carbonation as a possible CO₂ sequestration process. *Chem. Eng. Sci.* **2006**, *61*, 4242–4251.
30. Berger, R.L.; Klemm, W. Accelerated curing of cementitious systems by carbon dioxide: Part II. Hydraulic calcium silicates and aluminates. *Cem. Concr. Res.* **1972**, *2*, 647–652.
31. Shi, X.; Fay, L.; Peterson, M.; Yang, Z. Freeze-thaw damage and chemical change of a portland cement concrete in the presence of diluted deicers. *Mater. Struct.* **2010**, *43*, 933–946.
32. Wang, H.; Gao, X.; Liu, J. Effects of salt freeze-thaw cycles and cyclic loading on the piezoresistive properties of carbon nanofibers mortar. *Constr. Build. Mater.* **2018**, *177*, 192–201.
33. Wang, H.; Gao, X.; Liu, J. Coupling effect of salt freeze-thaw cycles and cyclic loading on performance degradation of carbon nanofiber mortar. *Cold Reg. Sci. Technol.* **2018**, *154*, 95–102.
34. Villain, G.; Thiery, M.; Platret, G. Measurement methods of carbonation profiles in concrete: Thermogravimetry, chemical analysis and gammadensimetry. *Cem. Concr. Res.* **2007**, *37*, 1182–1192.
35. Chang, C.F.; Chen, J.W. The experimental investigation of concrete carbonation depth. *Cem. Concr. Res.* **2006**, *36*, 1760–1767.
36. Lo, Y.; Lee, H. Curing effects on carbonation of concrete using a phenolphthalein indicator and Fourier-transform infrared spectroscopy. *Build. Environ.* **2002**, *37*, 507–514.
37. Liu, Q.; Iqbal, M.; Yang, J.; Lu, X.; Zhang, P.; Rauf, M. Prediction of chloride diffusivity in concrete using artificial neural network: Modelling and performance evaluation. *Constr. Build. Mater.* **2021**, *266*, 12108.
38. Mao, L.; Hu, Z.; Xia, J.; Feng, G.; Azim, I.; Yang, J.; Liu, Q. Multi-phase modelling of electrochemical rehabilitation for ASR and chloride affected concrete composites. *Compos. Struct.* **2019**, *207*, 176–189.